Human Molecular Genetics, 2012, Vol. 21, No. 12 **2807–2814**
doi:10.1093/hmg/dds108
Advance Access published on March 22, 2012

Severe disturbance in the Ca^{2+} signaling in astrocytes from mouse models of human infantile neuroaxonal dystrophy with mutated *Pla2g6*

Mikhail Strokin[1], Kevin L. Seburn[2], Gregory A. Cox[2], Kimberly A. Martens[2] and Georg Reiser[1,*]

[1]Institut für Neurobiochemie, Medizinische Fakultät, Otto-von-Guericke-Universität Magdeburg, Leipziger Straße 44, 39120 Magdeburg, Germany, and [2]The Jackson Laboratory, 600 Main Street, Bar Harbor, ME 04609, USA

Received January 31, 2012; Revised and Accepted March 14, 2012

Infantile neuroaxonal dystrophy (INAD; OMIM #no. 256600) is an inherited degenerative nervous system disorder characterized by nerve abnormalities in brain, spinal cord and peripheral nerves. About 85% of INAD patients carry mutations in the *PLA2G6* gene that encodes for a Ca^{2+}-independent phospholipase A_2 (VIA $iPLA_2$), but how these mutations lead to disease is unknown. Besides regulating phospholipid homeostasis, VIA $iPLA_2$ is emerging with additional non-canonical functions, such as modulating store-regulated Ca^{2+} entry into cells, and mitochondrial functions. In turn, defective Ca^{2+} regulation could contribute to the development of INAD. Here, we studied possible changes in ATP-induced Ca^{2+} signaling in astrocytes derived from two mutant strains of mice. The first strain carries a hypomorphic allele of the *Pla2g6* that reduces transcript levels to 5–10% of that observed in wild-type mice. The second strain carries a point mutation in *Pla2g6* that results in inactive VIA $iPLA_2$ protein with postulated gain in toxicity. Homozygous mice from both strains develop pathology analogous to that observed in INAD patients. The nucleotide ATP is the most important transmitter inducing Ca^{2+} signals in astroglial networks. We demonstrate here a severe disturbance in Ca^{2+} responses to ATP in astrocytes derived from both mutant mouse strains. The duration of the Ca^{2+} responses in mutant astrocytes was significantly reduced when compared with values observed in control cells. We also show that the reduced Ca^{2+} responses are probably due to a reduction in capacitative Ca^{2+} entry (2.3-fold). Results suggest that altered Ca^{2+} signaling could be a central mechanism in the development of INAD pathology.

INTRODUCTION

Human infantile neuroaxonal dystrophy (INAD; OMIM #no. 256600) is an inherited disease characterized by progressive motor and sensory impairment. Symptom onset occurs between 6 months and 2 years of age, followed by the loss of ambulation within 5 years. This type of the disease was designated as 'classic INAD' (1). A disease hallmark used in diagnosis is the presence of axonal spheroids in peripheral nerve biopsies (2). Some individuals with INAD show high brain iron, similar to the neurodegeneration with brain iron accumulation (NBIA). In some cases, signs and symptoms of INAD first appear late in childhood or during the teenage years and progress slowly, designated as 'atypical NAD' (1). Importantly, the pathology associated with mutations in *PLA2G6* exhibits a pathogenesis shared with both Parkinson's disease and Alzheimer's disease. Not only the peripheral and central spheroids, but also α-synuclein-positive Lewy bodies, dystrophic neurites and neurofibrillary tangles were detected in the brain tissue of a 23-year-old patient with atypical NAD (1).

Genome-wide linkage screening of the members of families with INAD revealed mutations on Chromosome 22q12-q13 in the gene encoding the group VIA Ca^{2+}-independent phospholipase A_2 (GenBank name *PLA2G6*) (3). However, the molecular mechanism of how the dysfunction of *PLA2G6* leads to the INAD phenotype has not been clarified. This enzyme is designated in the nomenclature as VIA $iPLA_2$ or $iPLA_2\beta$. More than 30 different phospholipases A_2 (PLA_2) have been identified so far in different mammalian cells (4), which emphasizes that the enzyme likely has multiple cell-specific

*To whom correspondence should be addressed. Tel: +49 3916713088; Fax: +49 3916713097; Email: georg.reiser@med.ovgu.de

functions. The major intracellular PLA_2 are classified into Ca^{2+}-dependent group IV PLA_2 ($cPLA_2$) and Ca^{2+}-independent group VI $iPLA_2$. About 70% of PLA_2 activity in the brain derives from group VI $iPLA_2$ (5), which is represented by two enzymes VIA $iPLA_2$ and VIB $iPLA_2$ that are encoded by different genes. A mutation in the VIA $iPLA_2$ gene (*PLA2G6*) was identified in the majority of INAD patients, and also in some of the NBIA (NBIA2A; OMIM #no. 256600) patients, and in patients with the related Karak syndrome (OMIM #no. 610217).

The primary role of VIA $iPLA_2$ activity in INAD has been suggested to involve disturbances in lipid homeostasis, lipid metabolism and structural abnormalities of cell or mitochondrial membranes (6). Yet, the evidence here is incomplete and the molecular mechanisms underlying INAD pathology are unknown.

A few investigations demonstrate that the VIA $iPLA_2$ regulates capacitative Ca^{2+} entry (CCE). CCE plays an important part in cellular Ca^{2+} homeostasis (7–9). CCE is a type of Ca^{2+} influx into the cells that occurs after emptying the Ca^{2+} stores in the endoplasmic reticulum (ER) observed after activation of Gq protein-coupled metabotropic receptors. The release of Ca^{2+} from the ER is activated by the second messenger inositol-1,4,5-trisphosphate ($InsP_3$) which is generated after hydrolysis of the membrane phospholipid phosphatidyl-4,5-bisphosphate by phospholipase C. A fall in Ca^{2+} concentration within the stores is sensed by stromal interaction molecule 1, which relays this change to Orai1, the pore-forming subunit of the Ca^{2+} release-activated Ca^{2+} channels (10). Functionally active VIA $iPLA_2$ has been shown to be essential for activation of Orai1 (11). Also *in situ*, this role of VIA $iPLA_2$ for CCE has been demonstrated in astrocytes using acute brain slices from rat cerebellum (12). We have shown that the inhibition of VIA $iPLA_2$ normalizes Ca^{2+} signaling in rat astrocytes under inflammatory conditions (9). These findings demonstrate the potential of VIA $iPLA_2$ as a pharmacological target that might be developed for INAD patients.

Animal models of INAD have emerged over the last several years beginning with two independently established knockout alleles of *Pla2g6* (13,14). However, these two mice should be considered as models for the atypical NAD characterized by late onset of the disease, because both mouse strains develop neurological symptoms merely in adult animals at 12–15 months of age and have only a slightly reduced lifespan.

More recently, two new mutant alleles were described that develop comparable INAD pathology but with a much earlier onset and faster progression (15,16). Mice carrying either of these spontaneous alleles develop overt motor deficits, hallmark INAD pathologies within several weeks after birth, and die prematurely ($\leq$6 months). In one case, the mice carry a severe hypomorphic allele of *Pla2g6* caused by a viral insertion upstream of the start codon (C3H/HeJ-Pla2g6^{m1J}/Rwb hereafter called VIA $iPLA_2$ hypomorph mice). This viral insertion dramatically reduces wild-type (WT) VIA $iPLA_2$ transcript level, without eliminating it totally. Thus, as there is no evidence of aberrant transcripts, this hypomorphic allele is presumed to operate as a simple loss-of-function. The second mouse strain carries a single-point mutation that results in a glycine to arginine exchange in a conserved amino acid at position 373 (G373R). This mutation is localized to a conserved ankyrin repeat domain of *PLA2G6* that was found to be mutated in INAD patients (3). Interestingly, in contrast to the VIA $iPLA_2$ hypomorph animals, these G373R animals display normal expression levels of both protein and mRNA. However, assay of the canonical VIA $iPLA_2$ activity in C57BL/6-Pla2g6^{m1Sein}/Rwb mice showed that the G373R mutation rendered the enzyme inactive (hereafter referred to as inactive VIA $iPLA_2$) (16). The presence of normal levels of mutant protein and the severity of the disease in mice carrying the G373R point mutation lead Wada and colleagues to propose a possible dominant-negative role for the mutant form of $iPLA_2$. However, the lack of a pathological phenotype in the heterozygous animals does not support this suggestion.

In the current work, we studied the possible molecular and mechanistic consequences of these different genetic defects in the *Pla2g6* gene by comparing the ATP-induced Ca^{2+} signaling in astrocytes derived from these two models of INAD. ATP is the most important transmitter for mediation of astrocyte Ca^{2+} signaling, which is implicated in gliotransmission. ATP propagates in the astrocytic network in the form of regenerative waves, which accompany the Ca^{2+} waves. ATP released from one astrocyte acts on purinergic ATP (P2Y) receptors on the neighboring cells (17).

We demonstrate a severe reduction in the duration of Ca^{2+} responses in ATP-stimulated astrocytes from both INAD strains. These changes in Ca^{2+} signaling arise due to the strong reduction in CCE. The effects were quite similar in both mice. Hence, our data support a new molecular mechanism for the development of INAD pathology and suggest that Gq-coupled receptor-induced Ca^{2+} signaling may provide a novel pharmacological target for this disorder.

RESULTS

A spontaneous mutation produces a novel model of INAD

The VIA $iPLA_2$ hypomorph mouse was identified in the C3H/HeJ production colony of The Jackson Laboratory based on the appearance of an overt motor deficit. The trait had a recessive inheritance pattern with no detectable phenotype in obligate heterozygotes. Initial mapping localized the mutation to mouse Chromosome 15 within a conserved region of synteny to human chromosome 22. Subsequent sequencing of candidate genes in the interval located a novel insertion of Intracisternal A Particle (IAP) [reviewed by Kuff and Lueders (18)] in intron 1 of the *Pla2g6* gene upstream of the start codon in exon 2 (Fig. 1A). To determine the effects of the insertion of this defective endogenous retrovirus, we examined the expression of VIA $iPLA_2$ mRNA in the brains of mutant mice using quantitative PCR. Results from three different amplicons spanning different exons showed that VIA $iPLA_2$ expression in homozygous mutants was $10 \pm 3\%$ of WT controls ($n = 3$ animals of each genotype). As there was no evidence of aberrant splice variants, we conclude that the $\sim$90% reduction in WT VIA $iPLA_2$ is caused by the IAP insertion and produces a severe loss-of-function allele.

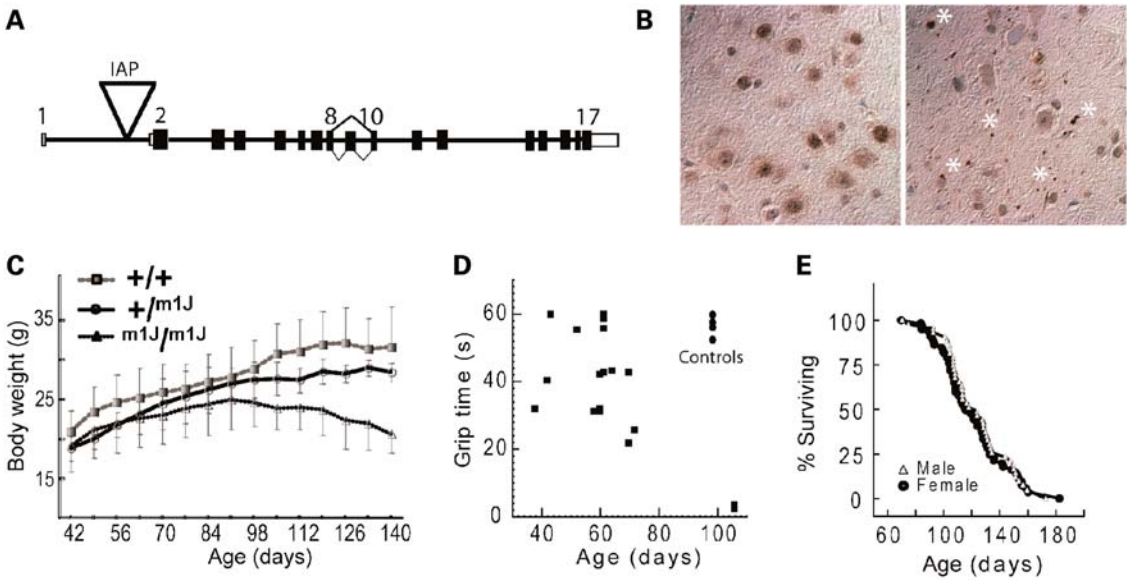

Figure 1. (**A**) Schematic of the 17 exon murine *Pla2g6* gene showing location of a viral Intracisternal A Particle (IAP) insertion at nucleotide position 15:79154430, 5989 bp upstream of Exon 2 and flanked by a 5 bp TCATC duplication. The orientation of the gene is shown inverted relative to that of the mouse reference sequence for Chromosome 15 (NCBI m37). (**B**) Ubiquitin-stained brain sections (substantia nigra) show that hypomorph VIA $iPLA_2$ mutants (right panel) have widespread ubiquitin-positive accumulations (spheroids) throughout the neuropil that are not present in littermate controls (left panel). Each asterisk indicates the location of one or more adjacent spheroids not associated with a cell body. Many smaller accumulations are visible throughout. Controls show only some background staining within visible cell bodies. (**C**) Growth curves for homozygous VIA $iPLA_2$ hypomorph mice (m1J/m1J) show a progressive decline in body weight that begins at about 90 days of age, while VIA $iPLA_2$ hypomorph heterozygotes (+/m1J) and control (+/+) littermates show typical steady increases ($n \geq 5$ all ages). (**D**) Mice were placed on a wire grid that was then inverted. Each mouse performed three trials with 1 min rest between trials. Points represent the average amount of time each mouse was able to stay on the inverted grid (60 s maximum). Note that 100-day-old WT controls (upper right of plot) can easily support their body weight for 50–60 s, while some VIA $iPLA_2$ hypomorph mice begin to perform poorly as early as 60 days of age and by ~100 days mutant mice are unable to sustain their grip for more than a few seconds. (**E**) Survival curves of male and female VIA $iPLA_2$ hypomorph homozygtes show a 50% survival of ~120 days and none of the mice survive beyond 6 months ($n = 43$ and 57, females and males, respectively). WT mice of this strain (data not shown) typically live greater than or equal to 2 years (http://phenome.jax.org).

Brain tissue from VIA $iPLA_2$ hypomorph mouse was examined for tubulovesicular accumulations referred to as 'spheroids'. The presence of spheroids in peripheral nerves of patients was a hallmark diagnostic prior to genetic testing. Consistent with INAD disease, late-stage mutants had widespread ubiquitinated accumulations throughout the neuropil of the brain that were not evident in age-matched controls (Fig. 1B). Mutant mice show normal increases in body weight until about 90 days of age when a gradual weight loss begins that continues until death (Fig. 1C). The appearance of a slight tremor is the first overt sign of disease in VIA $iPLA_2$ hypomorph mice and can be visually detected at ~50 days of age. As the disease develops, their performance on a wire-hang test declines. Mutants begin to lose the ability to hang suspended between 60–80 days and by 100 days, the animals no longer have sufficient grip strength to support their weight for more than a few seconds (Fig. 1D). The loss of grip strength is analogous to the early appearance of hypotonia in patients. Finally, although homozygous VIA $iPLA_2$ hypomorph mice are fertile, the animals rarely survive beyond 6 months of age and have a 50% survival of ~120 days (Fig. 1E).

The early disease onset, pathology, loss of grip strength and shortened lifespan of VIA $iPLA_2$ hypomorph mice are all consistent with descriptions of classic INAD in humans and therefore provide a novel model for the study of this childhood disease.

Augmented Ca^{2+} signaling in ATP-stimulated astrocytes from INAD mice

We first studied Ca^{2+} signaling in astrocytes from VIA $iPLA_2$ hypomorph mice. The cells were isolated from 6- to 8-week-old animals and cultured for 14–16 days. Then the cells were stimulated with ATP for 5 min. Compared with responses seen in cells from the WT animals, we observed a moderate reduction in the amplitudes of the responses. However, the duration of the response was drastically reduced in astrocytes from hypomorph mice (Fig. 2). The duration of the responses was estimated by measuring the peak width at the half-height of the response curve. This parameter reflects the time of exposure of the cells to the elevated intracellular Ca^{2+} concentrations. In the cells from hypomorph animals, the peak width of the ATP response curve comprised only 23% when compared with the results obtained in the cells from WT animals (Fig. 2C).

Reduction of CCE in astrocytes from mice VIA $iPLA_2$ hypomorph and VIA $iPLA_2$ inactive

Decreases in the amplitude and duration of Ca^{2+} responses could originate from a decrease in the CCE. CCE is activated upon Ca^{2+} release from the intracellular stores. To analyze the CCE, we stimulated astrocytes in the presence of Mn^{2+} in the superfusion buffer. Mn^{2+} passes through the same channels as

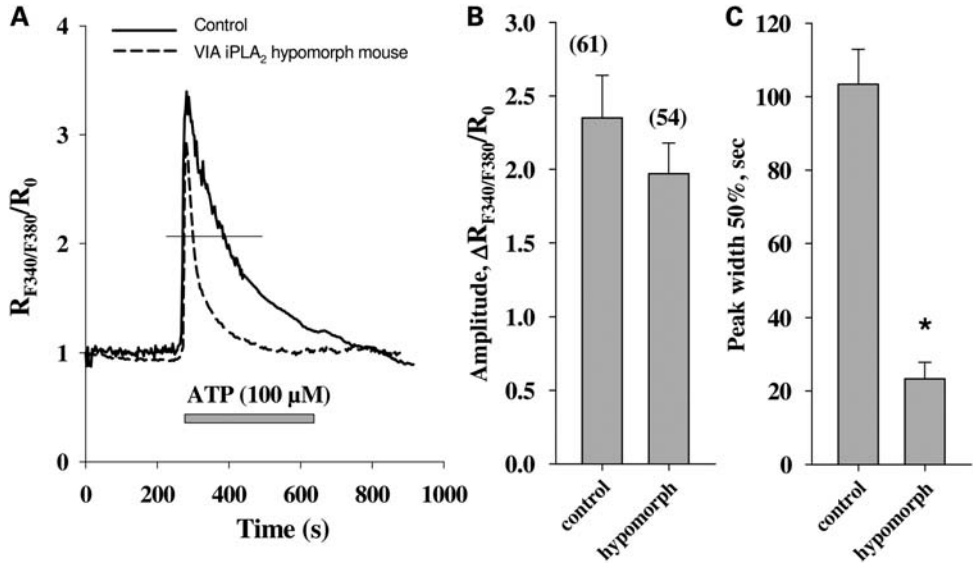

Figure 2. Ca^{2+} responses in ATP-stimulated astrocytes from normal (solid line) and VIA $iPLA_2$ hypomorph mice (dashed line). The traces are normalized to the Ca^{2+} concentration at the beginning of the experiment. The bar under the curves represents presence of the respective compound (ATP, 100 μM) in the superfusion buffer. The thin horizontal line demonstrates the response width at 50% of maximal amplitude. The amplitudes and peak width of the response curves at the half-height are presented in the panels (**B**) and (**C**), respectively. In panel (B), the numbers in parentheses give the total number of cells tested [also applicable for (C)]. The traces presented are the average traces from one experimental day. The values are the averages from at least six experiments from three different cell preparations (two experiments from one preparation). Asterisk means significantly different from the corresponding control value; 'control' value obtained for non-treated cells; $P < 0.05$.

Ca^{2+} and quenches the fluorescent dye Fura-2. Hence, the CCE can be estimated as the quenching rate of Fura-2. For this purpose, the Fura-2 fluorescence was detected using excitation light with a 360 nm wavelength, where the emission of Fura-2 is independent from the Ca^{2+} concentration. The slope of the experimental curve for fluorescence at 360 nm after the addition of ATP (100 μM) was taken as a quantitative characteristic of CCE (see Fig. 3 for details).

We found that ATP-induced CCE was strongly reduced in astrocytes from VIA $iPLA_2$ hypomorph mice (Fig. 3A). The CCE in cells from the VIA $iPLA_2$ hypomorph animals amounted to only 45% of the value obtained for the control WT cells (Fig. 3B). Remarkably, we obtained essentially the same results in cells from mice with inactive VIA $iPLA_2$ (Fig. 3C and D). The CCE in astrocytes from mice with inactive VIA $iPLA_2$ was reduced by 43% (Fig. 3D).

In order to understand the mechanism responsible for changes in Ca^{2+} signaling, we compared the alterations observed in animals with reduced VIA $iPLA_2$ expression or with inactive VIA $iPLA_2$ with those induced by pharmacological inhibition of VIA $iPLA_2$ (Fig. 3D). Importantly, the treatment of the cells from the mice with inactive VIA $iPLA_2$ with S-BEL did not influence the ATP-induced CCE. Notably, the CCE in astrocytes from VIA $iPLA_2$ hypomorph mice was not affected further by treatment with S-BEL (Fig. 3B).

We could mimic the CCE reduction by pharmacological inhibition of VIA $iPLA_2$ with S-BEL (2.5 μM for 30 min) in WT cells. These data confirm that the change in Ca^{2+} response in the VIA $iPLA_2$ is due to reduced activity of the VIA $iPLA_2$ protein and not because of the deficit in the VIA $iPLA_2$ protein level.

DISCUSSION

In this study, we investigated the consequences of defects in the VIA $iPLA_2$ gene (*Pla2g6*) for ATP-induced Ca^{2+} signaling in astrocytes. These mice are excellent models of the inherited neurodegenerative disease INAD as they display an early onset of neuroaxonal dystrophy with overt motor dysfunction by 2–3 months and premature death by 6 months of age. In contrast, the full knock-out *Pla2g6* mice exhibit very late onset of the disease phenotype and almost normal life span (13,14), which is characteristic for the atypical NAD (1). One mouse is a severe hypomorph for WT VIA $iPLA_2$ and the other expresses normal levels of a lipase-inactive mutant form of VIA $iPLA_2$ (16).

Here, we demonstrate a severe disturbance in ATP-stimulated Ca^{2+} signaling in astrocytes derived from both INAD mouse strains. To our knowledge, this is the first report to explore changes in Ca^{2+} signaling from cells with INAD mutations. We find that astrocytes from mice with different *Pla2g6* mutations show a similar effect. The duration of the Ca^{2+} responses to ATP is significantly shorter than in the cells from control animals. This is consistent with the phenotypic similarity of these two alleles in the timing of disease onset, INAD pathology and mortality for these two *Pla2g6* mutant mice (this report and (16)). Our finding suggests that astrocytic dysfunction may be a common mechanism leading to general nervous system collapse. The altered Ca^{2+} response to ATP is most likely due to the strong reduction in CCE, which is activated after the emptying of ER Ca^{2+} stores by purinergic receptor challenge. This conclusion is strongly supported by the observation that the amplitude of the primary

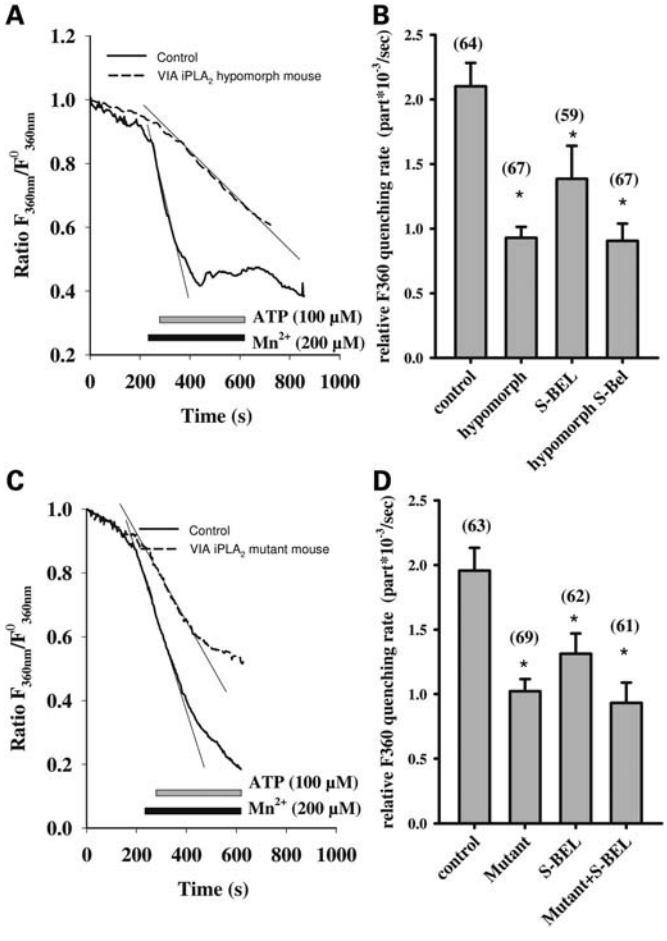

Figure 3. CCE reduction in astrocytes from VIA $iPLA_2$ hypomorph mice (**A**, **B**) and mice with inactive VIA $iPLA_2$ (**C**, **D**). Experimental traces for astrocytes from hypomorph mice (A), mice with inactive VIA iPLA (C) (dashed lines) when compared with WT mice (solid lines) show the fluorescence ratio of Fura-2 with excitation at 360 nm. The traces are normalized to the fluorescence at the beginning of the experiment. The horizontal bars under the curves represent the presence of the respective compounds (ATP, Mn^{2+}) in the superfusion buffer. The CCE rate is presented as Fura-2 quenching rate in panel (B) for VIA $iPLA_2$ hypomorph mice and in panel (D) for mice with inactive VIA $iPLA_2$. The quenching rate was estimated as slope (thin tangential lines on the graphs) of the curves in the presence of both ATP and Mn^{2+} minus the slope in the presence of Mn^{2+} only (A, C). In panels (B) and (D), the numbers in parentheses give the total number of cells tested. S-BEL (2.5 μM) was given, when appropriate for 30 min prior to the measurements of the fluorescence. The traces presented are the average traces from one experimental day. The values are the averages from at least six experiments from three different cell preparations (two experiments from one preparation). 'Control' value is obtained from non-treated cells. Asterisk means significantly different from the corresponding control value, $P < 0.05$.

response to ATP in the *Pla2g6* mutant mice tested here remained virtually unaffected in comparison with the response seen in astrocytes from control animals. This means that comparable amounts of Ca^{2+} were released from the stores, yet the following Ca^{2+} influx rate was reduced in cells from *Pla2g6* mutant mice (Fig. 3).

The effects of the genetic reduction of VIA $iPLA_2$ are corroborated by the pharmacological results. We could mimic the reduced CCE observed in VIA $iPLA_2$ mutant mice by pharmacological inhibition of VIA $iPLA_2$ in control animals. The CCE observed after inhibition of VIA $iPLA_2$ with S-BEL in cells from control animals was somewhat higher than the CCE observed in both mutant mice strains. This could be a consequence of adaptation of cells in mutant animals, which results in slightly different response patterns. Importantly, the similarity of the results in both strains, either hypomorphic for WT VIA $iPLA_2$ or expressing mutant-inactive VIA $iPLA_2$, demonstrates that the observed effects are likely caused by loss of the VIA $iPLA_2$ activity. Wada and colleagues (16) proposed a possible gain of function caused by the point mutation (G373R) that may accelerate the disease. This hypothesis was not tested, but our results, at least with regard to astrocytic function, argue against a toxic gain-of-function because astrocytes derived from both mutant strains function similarly.

Our results are in good agreement with indications that VIA $iPLA_2$ controls Ca^{2+} influx into the cells via CCE (7–9,12). The reduction of CCE in astrocytes after reduction of $iPLA_2$ activity should be universal for Gq protein-coupled receptors for different agonists, as CCE is activated generally after Ca^{2+} release from the ER. For example, we observed in rat primary astrocytes that inhibition of VIA $iPLA_2$ by S-BEL produced comparable reduction of CCE after stimulation of the cells with either ATP or glutamate (our own unpublished observations). This makes our present results especially interesting, since activation of Ca^{2+} responses in astrocytes by different neurotransmitters released at the synapse is an essential part of neuron–astrocyte communication (19,20). Importantly, we have shown previously that increased expression of VIA $iPLA_2$ enhances CCE and Ca^{2+} responses (9). Here, we show that suppression of VIA $iPLA_2$ expression lessens the Ca^{2+} responses in astrocytes. These data highlight the central role of VIA $iPLA_2$ in the regulation of Ca^{2+} homeostasis in astrocytes.

Calcium as a second messenger system influences enzymes, ion channels and cytoskeletal elements. It also controls gene transcription (21). A significant portion of the executive features of astrocytes, i.e. the production of immunoregulatory and neuroregulatory cytokines and chemokines, depends on the *de novo* synthesis of proteins. In recent years, a large body of evidence has been accumulated suggesting that astrocytes play a central role in numerous cooperative metabolic processes with neurons (reviewed in earlier studies (19,22)). Moreover, astrocytes influence neurotransmission itself by the formation of tripartite synapses (20). Impairments of astrocytic functions are increasingly recognized as an important contributor to neuronal dysfunction and, in particular, neurodegenerative processes (23). Hence, the correct Ca^{2+} signaling in the astroglial network is crucial for sustained functioning of the neural tissue as whole.

The link between different pathological states in the brain and changes in activity and expression of different PLA_2 isoforms (24,25) suggest that PLA_2 components are potential pharmacological targets for treatment of neurodegenerative diseases. $cPLA_2$ and $iPLA_2$ have been shown to be involved in amyloid-β peptide-induced mitochondrial dysfunction in astrocytes (26) and amyloid-induced damage to neurons (27). $iPLA_2$ was shown to mediate ischemic damage in brain (28). $cPLA_2$ is able to sense the Ca^{2+} signals and reactive oxygen species in brain cells, and thereby initiates the

generation of a number of inflammatory lipid mediators (24). Yet, both cPLA$_2$ and iPLA$_2$ are constitutively expressed in brain. Their activities have been shown to be crucial for neurite outgrowth and neuronal viability (29,30). Therefore, the exact role of distinct isoforms of PLA$_2$ enzymes and the consequences of possible medical treatment have yet to be precisely elucidated.

VIA iPLA$_2$ is accepted to regulate Ca^{2+} influx into the cells through CCE channels located on the cell plasma membrane. However, iPLA$_2$ was shown to be located also in mitochondria, where it can affect the mitochondrial Ca^{2+} uptake (31). Mitochondrial Ca^{2+} uptake, in turn, is important for store-dependent Ca^{2+} entry and store refilling (32,33). Inhibition of VIA iPLA$_2$ could lead to the reduced mitochondrial Ca^{2+} processing and capacity (9). Moreover, VIA iPLA$_2$ was found to protect mitochondria in INS-1 insulinoma cells from staurosporine-induced decrease of the membrane potential, and release of cytochrome c and apoptosis-inducing factor (34). Hence, the disturbance in Ca^{2+} signaling in astrocytes from mice with reduced or inactive VIA iPLA$_2$ may also arise from malfunctioning mitochondria. Additionally, a recent study reported that distal axons in the brain of VIA iPLA$_2$-null mice contained mitochondria with degenerative inner membranes. The abnormal mitochondria were observed adjacent to regions of degenerating cytoskeleton in presynaptic membranes (6) and led the authors to propose that the absence of VIA iPLA$_2$ caused insufficient membrane remodeling at these locations, hence referring to the classical role of VIA iPLA$_2$ as a phospholipase. However, the timing and nature of the presumed mitochondrial dysfunction were not investigated. This issue clearly requires further study.

Finally, it is also worth noting that as studies of INAD advance, some caution may be warranted in considering experimental results using available mouse models. For instance, knockout models described in the literature (13,14) have a greatly delayed onset of neurological symptoms (~1 year) and a near-normal lifespan (~1.5 years) compared with the two mouse strains used in this study (15,16), which have similar early onset (2–3 months) and premature death (6 months). The possible explanation could be that knockout mice, which express no VIA iPLA$_2$, have triggered a compensatory pathway. However, such compensatory mechanisms remain inactive in animals used in this study expressing either low levels of WT VIA iPLA$_2$ or normal levels of a functionally inactive enzyme. Importantly, the similar early onset of INAD symptoms and the reduced lifespan of VIA iPLA$_2$ hypomorph and inactive VIA iPLA$_2$ mice indicate that rapid pathology development does not result from the increased toxicity of VIA iPLA$_2$ with point mutation (G373) as Wada *et al*. (16) proposed in their original work.

In conclusion, we demonstrate that defects in the iPLA$_2$ gene evoke severe Ca^{2+} signaling disturbances in astrocytes, suggesting that possible treatment strategies normalizing Ca^{2+} homeostasis may be beneficial. Furthermore, the role of iPLA$_2$ in mitochondrial functionality can be an additional direction for understanding INAD pathogenesis, since mitochondria dysfunction is a common hallmark for a number of neurodegenerative diseases, including Alzheimer's and Parkinson's diseases.

MATERIALS AND METHODS

qPCR protocol

Brain tissue from three WT and three VIA iPLA$_2$ hypomorph mice was isolated and mRNA was extracted (RNEasy, Qiagen Kit 74104) and used to make cDNA according to the manufacturer's instructions (Supersript III, Invitrogen Kit 18080-051). Primer sets were validated by confirming linearity across a dilution series using control cDNA, and a dissociation curve confirmed the presence of a single product for each primer pair. Primers were premixed to a final concentration of 0.2 μM and combined with 10 ng cDNA in dH$_2$O and Sybr Green Master mix (Applied Biosystems) in a 96-well plate for reaction and measurement (ABI 7500; Applied Biosystems).

Gapdh (glyceraldehyde 3-phosphate dehydrogenase) was used as a reference and ΔCt for each *Pla2g6* primer set for each animal was calculated as: $Ct^{Pla2g6} - Ct^{Gapdh}$ and mutant *Pla2g6* expression was calculated as $2^{(WT\Delta Ct - Mutant\Delta Ct)}$. Reported values are the average of three animals for each group across all three primer sets. Three different primer sets spanning exons 1–2, 11–12 and 16–17 were used. Primer sequences 5′–3′: Exon1F-GTCACCTGGACCCTGCT TAG; Exon2R-TGACGCTACTGAGGGTGTTG; Exon11F-ACCAAGGACCTCTTCGACTG; Exon12R-AAACTCCCGC TTCAGGAACT; Exon16F-GAGATGGTCGGCATCCAGTA; Ex17R-GAACTCCTCTCGGTGCTCAT.

Mice genotyping

DNA was extracted from tail tips by overnight incubation at 50°C in 100 μl of tail buffer (100 mM Tris, 200 mM NaCl, 5 mM EDTA, pH 8.5) with 12.5 μl proteinase K (10 mg/ml) and then boiled for 15 min. The mutations were analyzed by PCR. For the analysis of hypomorph mutation, common forward (TGT GGC ATC TCT GGC TGG AAA C), mutant reverse (GGC TCA TGC GCA GAT TAT TT) and WT reverse (CCA GGC AGG AAT GCT ACA AAG C) primers were used. PCR was performed in 20 μl reaction mixture containing 10 Taq mastermix (Invitrogen), 1 μl DNA (sample), primers at final concentration 0.2 μM. PCR protocol: 94°C–25 s, 57°C–30 s, 72°C–30 s, 34 cycles. Electrophoresis was performed in 2% gel. The mutant band runs at 150 bp, and the WT band at 300 bp, respectively. The VIA iPLA$_2$ inactive mutation was analyzed by performing separate PCR reactions for each WT and mutant allele, using common forward (CCT GTG GAA GAG CAG AGG G) primer, WT reverse (GGT GTC CAC TTC TGC CCC A) and mutant reverse (GGT GTC CAC TTC TGC CCT A) primers. PCR protocol: 94°C–25 s, 62.5°C–30 s, 72°C–30 s, 34 cycles. Electrophoresis was performed in 2% agarose gel. The band in both cases runs at ~200 bp.

Cell cultures

Whole-brain astrocytes and neurons were prepared from 6- to 8-week-old mice. After decapitation, meninges were removed and the brains were minced into small pieces using a surgical scalpel. Brain pieces were transferred into sterile falcon tubes, washed twice with ice-cold preparation medium, which

contained 1 mM pyruvate, 10 mM glucose, 6 μg/ml DNAse I type IV, 1 mg/ml bovine serum albumin, 2 mM stabilized glutamine and antibiotics mixture (penicillin, 100 U/ml and streptomycin, 0.1 mg/ml) in a Ca^{2+}-free HEPES-buffered salt solution (10 mM HEPES, pH 7.2). Brain pieces were digested in preparation medium supplemented with 4 mg/ml trypsin type XI for 7 min at 37°C. Digestion was stopped by adding RPMI-1640 medium (Biochrom; 10% heat-inactivated fetal calf serum, 100 U/ml penicillin, 10 μg/ml streptomycin) and pieces were triturated after washing with preparation medium. The cell suspension was filtered by a tube-top cell strainer (pore size 100 μm BD Biosciences) and centrifuged for 5 min at 500*g*. Then, the cells were resuspended in RPMI-1640 medium (10% heat-inactivated fetal calf serum, 100 U/ml penicillin, 10 μg/ml streptomycin) and seeded on round coverslips (22 mm diameter) placed in culture dishes (50 mm diameter). First medium change is done on third day in culture, second on eighth day in culture and then after every second day. The cells were taken for further work after 14–16 days in culture.

Cytosolic Ca^{2+} measurements

The concentration of free intracellular Ca^{2+} ($[Ca^{2+}]_i$) was measured using the Ca^{2+}-sensitive fluorescent dye Fura-2/AM. For dye loading, the cells grown on a coverslip were placed in 1 ml HEPES-buffered saline [HBS; buffer composition in millimolars: 145 NaCl, 5.4 KCl, 1 $MgCl_2$, 1.8 $CaCl_2$, 25 glucose, 20 HEPES, pH 7.4 adjusted with Tris] for 30 min at 37°C, supplemented with 3 μM Fura-2/AM (Invitrogen). Loaded cells were transferred into a perfusion chamber with a bath volume of about 0.2 ml and mounted on an inverted microscope (Zeiss, Axiovert 135). During the experiments, the cells were continuously superfused with medium heated to 37°C.

Single cell fluorescence measurements of $[Ca^{2+}]_i$ were performed using an imaging system from T.I.L.L. Photonics GmbH. Cells were excited alternately at 340, 360 and 380 nm for 50–70 ms at each wavelength with a rate of 0.33 Hz and the resultant emission was collected above 510 nm. Images were stored on a computer and subsequently the changes in fluorescence ratio (F_{340}/F_{380}) were determined from selected regions of interest covering a single cell. Fluorescence ratios were compared from the same day measurement.

Statistics

Every experimental protocol was performed in one experiment using at least two different coverslips with cells from the same culture. Then replica experiments were carried out using cells from another preparation. Mean values for the indicated number of cells are presented. Data were subjected to an ANOVA with Tukey's post hoc comparison or to Student's *t*-test if only two datasets were compared. Statistical significance was established at $P < 0.05$.

ACKNOWLEDGEMENTS

We thank A. Schneider and P. Grüneberg for technical support with animals, cell cultures and genotyping.

Conflict of Interest statement: None declared.

FUNDING

The work in the contributing author's laboratory (G.R.) was funded by grants from Deutsche Forschungsgemeinschaft (DFG; Re563/15-1) and Bundesministerium für Bildung und Forschung (BMBF; RUS 09/030); K.A.M. were supported by an MDA Development Grant; G.A.C. and K.L.S. were supported in part by NIH grant AR054170 and NS054154.

REFERENCES

1. Gregory, A., Westaway, S.K., Holm, I.E., Kotzbauer, P.T., Hogarth, P., Sonek, S., Coryell, J.C., Nguyen, T.M., Nardocci, N., Zorzi, G. *et al.* (2008) Neurodegeneration associated with genetic defects in phospholipase A_2. *Neurology*, **71**, 1402–1409.
2. Nardocci, N., Zorzi, G., Farina, L., Binelli, S., Scaioli, W., Ciano, C., Verga, L., Angelini, L., Savoiardo, M. and Bugiani, O. (1999) Infantile neuroaxonal dystrophy: clinical spectrum and diagnostic criteria. *Neurology*, **52**, 1472–1478.
3. Morgan, N.V., Westaway, S.K., Morton, J.E., Gregory, A., Gissen, P., Sonek, S., Cangul, H., Coryell, J., Canham, N., Nardocci, N. *et al.* (2006) *PLA2G6*, encoding a phospholipase A_2, is mutated in neurodegenerative disorders with high brain iron. *Nat. Genet.*, **38**, 752–754.
4. Burke, J.E. and Dennis, E.A. (2009) Phospholipase A_2 structure/function, mechanism, and signaling. *J. Lipid Res.*, **50** (Suppl), S237–S242.
5. Yang, H.C., Mosior, M., Ni, B. and Dennis, E.A. (1999) Regional distribution, ontogeny, purification, and characterization of the Ca^{2+}-independent phospholipase A_2 from rat brain. *J. Neurochem.*, **73**, 1278–1287.
6. Beck, G., Sugiura, Y., Shinzawa, K., Kato, S., Setou, M., Tsujimoto, Y., Sakoda, S. and Sumi-Akamaru, H. (2011) Neuroaxonal dystrophy in calcium-independent phospholipase $A_2\beta$ deficiency results from insufficient remodeling and degeneration of mitochondrial and presynaptic membranes. *J. Neurosci.*, **31**, 11411–11420.
7. Itagaki, K., Menconi, M., Antoniu, B., Zhang, Q., Gonnella, P., Soybel, D., Hauser, C. and Hasselgren, P.O. (2010) Dexamethasone stimulates store-operated calcium entry and protein degradation in cultured L6 myotubes through a phospholipase A_2-dependent mechanism. *Am. J. Physiol. Cell. Physiol.*, **298**, C1127–C1139.
8. Csutora, P., Peter, K., Kilic, H., Park, K.M., Zarayskiy, V., Gwozdz, T. and Bolotina, V.M. (2008) Novel role for STIM1 as a trigger for calcium influx factor production. *J. Biol. Chem.*, **283**, 14524–14531.
9. Strokin, M., Sergeeva, M. and Reiser, G. (2011) Proinflammatory treatment of astrocytes with lipopolysaccharide results in augmented Ca^{2+} signaling through increased expression of via phospholipase A_2 ($iPLA_2$). *Am. J. Physiol. Cell. Physiol.*, **300**, C542–C549.
10. Chang, W.C. and Parekh, A.B. (2004) Close functional coupling between Ca^{2+} release-activated Ca^{2+} channels, arachidonic acid release, and leukotriene C4 secretion. *J. Biol. Chem.*, **279**, 29994–29999.
11. Yang, B., Gwozdz, T., Dutko-Gwozdz, J. and Bolotina, V.M. (2011) Orai1 and Ca^{2+}-independent phospholipase A_2 are required for store-operated IcatSOC current, Ca^{2+} entry and proliferation of primary vascular smooth muscle cell. *Am. J. Physiol. Cell. Physiol.*, **302**, C748–C756.
12. Singaravelu, K., Lohr, C. and Deitmer, J.W. (2006) Regulation of store-operated calcium entry by calcium-independent phospholipase A_2 in rat cerebellar astrocytes. *J. Neurosci.*, **26**, 9579–9592.
13. Malik, I., Turk, J., Mancuso, D.J., Montier, L., Wohltmann, M., Wozniak, D.F., Schmidt, R.E., Gross, R.W. and Kotzbauer, P.T. (2008) Disrupted membrane homeostasis and accumulation of ubiquitinated proteins in a mouse model of infantile neuroaxonal dystrophy caused by PLA2G6 mutations. *Am. J. Pathol.*, **172**, 406–416.
14. Shinzawa, K., Sumi, H., Ikawa, M., Matsuoka, Y., Okabe, M., Sakoda, S. and Tsujimoto, Y. (2008) Neuroaxonal dystrophy caused by group VIA phospholipase A_2 deficiency in mice: a model of human neurodegenerative disease. *J. Neurosci.*, **28**, 2212–2220.
15. Seburn, K.L., Huebsch, K., Bogdanik, L., Burgess, R.W. and Cox, G.A. (2009) Peripheral nerve and neuromuscular junction defects in a mouse model of infantile neuroaxonal dystrophy. *Neuroscience 2009* (Online).
16. Wada, H., Yasuda, T., Miura, I., Watabe, K., Sawa, C., Kamijuku, H., Kojo, S., Taniguchi, M., Nishino, I., Wakana, S. *et al.* (2009) Establishment of an improved mouse model for infantile neuroaxonal

dystrophy that shows early disease onset and bears a point mutation in *Pla2g6*. *Am. J. Pathol.*, **175**, 2257–2263.
17. Guthrie, P.B., Knappenberger, J., Segal, M., Bennett, M.V., Charles, A.C. and Kater, S.B. (1999) ATP released from astrocytes mediates glial calcium waves. *J. Neurosci.*, **19**, 520–528.
18. Kuff, E.L. and Lueders, K.K. (1988) The intracisternal A-particle gene family: structure and functional aspects. *Adv. Cancer Res.*, **51**, 183–276.
19. Verkhratsky, A., Krishtal, O.A. and Burnstock, G. (2009) Purinoceptors on neuroglia. *Mol. Neurobiol.*, **39**, 190–208.
20. Halassa, M.M. and Haydon, P.G. (2010) Integrated brain circuits: astrocytic networks modulate neuronal activity and behavior. *Annu. Rev. Physiol.*, **72**, 335–355.
21. Berridge, M.J., Bootman, M.D. and Roderick, H.L. (2003) Calcium signalling: dynamics, homeostasis and remodelling. *Nat. Rev. Mol. Cell Biol.*, **4**, 517–529.
22. Allaman, I., Belanger, M. and Magistretti, P.J. (2011) Astrocyte-neuron metabolic relationships: for better and for worse. *Trends Neurosci.*, **34**, 76–87.
23. Parpura, V., Heneka, M.T., Montana, V., Oliet, S.H., Schousboe, A., Haydon, P.G., Stout, R.F. Jr., Spray, D.C., Reichenbach, A., Pannicke, T. *et al.* (2012) Glial cells in (patho)physiology. *J. Neurochem.*, **121**, 4–27.
24. Sun, G.Y., Horrocks, L.A. and Farooqui, A.A. (2007) The roles of NADPH oxidase and phospholipases A_2 in oxidative and inflammatory responses in neurodegenerative diseases. *J. Neurochem.*, **103**, 1–16.
25. Sun, G.Y., Shelat, P.B., Jensen, M.B., He, Y., Sun, A.Y. and Simonyi, A. (2010) Phospholipases A2 and inflammatory responses in the central nervous system. *Neuromolecular Med.*, **12**, 133–148.
26. Zhu, D., Lai, Y., Shelat, P.B., Hu, C., Sun, G.Y. and Lee, J.C. (2006) Phospholipases A_2 mediate amyloid-beta peptide-induced mitochondrial dysfunction. *J. Neurosci.*, **26**, 11111–11119.
27. Lee, J.C., Simonyi, A., Sun, A.Y. and Sun, G.Y. (2011) Phospholipases A_2 and neural membrane dynamics: implications for Alzheimer's disease. *J. Neurochem.*, **116**, 813–819.
28. Strokin, M., Chechneva, O., Reymann, K.G. and Reiser, G. (2006) Neuroprotection of rat hippocampal slices exposed to oxygen-glucose deprivation by enrichment with docosahexaenoic acid and by inhibition of hydrolysis of docosahexaenoic acid-containing phospholipids by calcium independent phospholipase A_2. *Neuroscience*, **140**, 547–553.
29. Forlenza, O.V., Mendes, C.T., Marie, S.K. and Gattaz, W.F. (2007) Inhibition of phospholipase A_2 reduces neurite outgrowth and neuronal viability. *Prostaglandins Leukot. Essent. Fatty Acids*, **76**, 47–55.
30. Mendes, C.T., Gattaz, W.F., Schaeffer, E.L. and Forlenza, O.V. (2005) Modulation of phospholipase A_2 activity in primary cultures of rat cortical neurons. *J. Neural Transm.*, **112**, 1297–1308.
31. Gadd, M.E., Broekemeier, K.M., Crouser, E.D., Kumar, J., Graff, G. and Pfeiffer, D.R. (2006) Mitochondrial $iPLA_2$ activity modulates the release of cytochrome c from mitochondria and influences the permeability transition. *J. Biol. Chem.*, **281**, 6931–6939.
32. Manjarres, I.M., Alonso, M.T. and Garcia-Sancho, J. (2011) Calcium entry-calcium refilling (CECR) coupling between store-operated Ca^{2+} entry and sarco/endoplasmic reticulum Ca^{2+}-ATPase. *Cell Calcium*, **49**, 153–161.
33. Malli, R., Frieden, M., Osibow, K., Zoratti, C., Mayer, M., Demaurex, N. and Graier, W.F. (2003) Sustained Ca^{2+} transfer across mitochondria is essential for mitochondrial Ca^{2+} buffering, store-operated Ca^{2+} entry, and Ca^{2+} store refilling. *J. Biol. Chem.*, **278**, 44769–44779.
34. Seleznev, K., Zhao, C., Zhang, X.H., Song, K. and Ma, Z.A. (2006) Calcium-independent phospholipase A_2 localizes in and protects mitochondria during apoptotic induction by staurosporine. *J. Biol. Chem.*, **281**, 22275–22288.